JCTC Journal of Chemical Theory and Computation

Article

Cite This: J. Chem. Theory Comput. 2018, 14, 3083−3090

pubs.acs.org/JCTC

Nonempirical Meta-Generalized Gradient Approximations for Modeling Chemisorption at Metal Surfaces

Alejandro J. Garza,[†] Alexis T. Bell,[*,‡] and Martin Head-Gordon[*,¶]

[†]Joint Center for Artificial Photosynthesis, Lawrence Berkeley National Laboratory, Berkeley, California 94720, United States

[‡]Department of Chemical and Biomolecular Engineering, University of California at Berkeley, Berkeley, California 94720, United States

[¶]Department of Chemistry, University of California at Berkeley, Berkeley, California 94720, United States

ABSTRACT: We assess the accuracy of popular nonempirical GGAs (PBE, PBEsol, RPBE) and meta-GGAs (TPSS, revTPSS, and SCAN) for describing chemisorption reactions at metal surfaces. Except for RPBE, all the functionals tend to overbind the adsorbate significantly. We then propose a nonempirical meta-GGA, denoted as RTPSS, that is based on RPBE in the same way that TPSS is based on PBE. The RTPSS functional remedies the overbinding problem and improves the description of chemisorption energies. As an example of an application of RTPSS, we study the adsorption of CO on Cu surfaces (a notably difficult problem for semilocal functionals) and find that RTPSS is the only tested functional that predicts accurate chemisorption energies and the preferred adsorption site of CO. Although RTPSS gives an accurate description of chemisorption, nonlocal correlation may be necessary to describe physisorption if long-range van der Waals interactions are involved (however, this is true for semilocal functionals in general). We suggest that RTPSS can be a useful meta-GGA for studying chemisorption processes and mechanisms of heterogeneous catalysis.

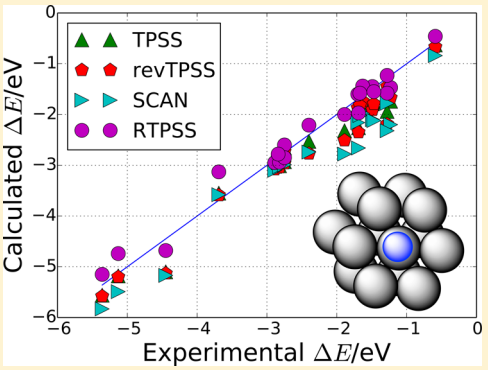

INTRODUCTION

In heterogeneous catalysis, the activity of a solid (typically metallic) catalyst is often determined by its ability to chemisorb reaction intermediates. For example, the high overpotentials required in the electroreduction of CO_2 to hydrocarbons and alcohols on copper are the result of inadequate chemisorption energies of key intermediates.[1] More generally, the importance of adsorption is reflected in the Sabatier principle,[2,3] which states that the interactions between the catalyst and the substrate cannot be either too weak or too strong for a reaction to take place. Therefore, theoretical methods that can accurately describe adsorption—in particular chemisorption—at metal surfaces are important in heterogeneous catalysis.

The high computational cost of evaluating Hartree−Fock exchange integrals for extended solids means that semilocal density functional approximations (DFAs) are often the tool of choice for modeling heterogeneous catalysts. Furthermore, semilocal functionals give a more realistic description of metals than hybrids.[4−6] However, popular semilocal DFAs such as the Perdew−Burke−Ernzerhof[7] (PBE) generalized gradient approximation (GGA) are known to predict chemisorption energies that are too negative with respect to experimental reference data.[8] This problem is rooted in the PBE exchange enhancement factor, F_x^{PBE}, that multiplies the exchange energy density of the uniform electron gas, ϵ_x

$$E_x^{\mathrm{PBE}} = \int F_x^{\mathrm{PBE}}(s)\epsilon_x(n)\,\mathrm{d}r = -\frac{3}{4}\left(\frac{3}{\pi}\right)^{1/3}\int F_x^{\mathrm{PBE}}(s)n(r)^{4/3}\,\mathrm{d}r \quad (1)$$

and that is defined as

$$F_x^{\mathrm{PBE}}(s) = 1 + \kappa - \frac{\kappa}{1 + \mu s^2/\kappa} \quad (2)$$

where s is the reduced density gradient

$$s = |\nabla n|/[2(3\pi^2)^{1/3}n^{4/3}] \quad (3)$$

and $\kappa = 0.804$ to ensure satisfaction of the Lieb−Oxford bound.[9,10] The value of s is typically largest at surface boundary regions; thus, s becomes smaller on average when a molecule adsorbs on a surface. This loss of regions of high s upon adsorption is illustrated in Figure 1. At s values typically relevant for chemisorption, F_x^{PBE} increases too slowly with s resulting in an overly strong preference for chemisorption. This observation motivated the use of an exchange enhancement factor that increases more rapidly with s in the revised PBE (RPBE) functional of Hammer et al.[8]

$$F_x^{\mathrm{RPBE}}(s) = 1 + \kappa(1 - \mathrm{e}^{-\mu s^2/\kappa}) \quad (4)$$

Received: March 23, 2018
Published: May 10, 2018

DOI: 10.1021/acs.jctc.8b00288
J. Chem. Theory Comput. 2018, 14, 3083−3090

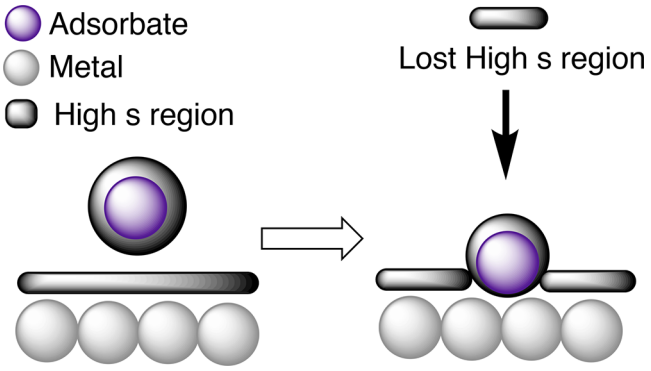

Figure 1. Schematic representation of an adsorption process illustrating the loss of regions of high reduced density gradient(s) upon chemisorption.

Both PBE and RPBE satisfy the same exact constraints. Although certain predicted properties are less accurate compared to PBE, RPBE yields significantly better chemisorption energies.

In an unrestricted Kohn−Sham framework at the semilocal level, meta-GGAs are potentially the most accurate type of functional.[11] In addition to the dependence on n and s, meta-GGAs use information from the orbital kinetic energy density, $\tau(r) = (1/2)\sum_i|\nabla\phi_i|^2$, that allows them to satisfy more exact constraints, differentiate between different types of bonds (covalent, metallic, or weak),[12] and better describe inhomogeneous systems in general. Only slightly more expensive than GGAs, meta-GGAs are affordable for modeling extended solids. Despite these advantages, meta-GGAs are not as widely used as GGAs for modeling heterogeneous systems. This has been in part due to historical inertia and in part due to the fact that meta-GGAs have not been shown to decisively outperform GGAs in describing, e.g., chemisorption and other surface properties. Hence, the development and benchmarking of meta-GGAs is of great potential interest in computational catalysis.

This work is focused precisely on that benchmark and development of meta-GGAs for applications in heterogeneous catalysis. To limit the scope of this study, we largely restrict ourselves to the computation of chemisorption energies with nonempirical meta-GGAs. Here, we should clarify that by nonempirical functionals we refer to DFAs of the school of thought championed by John Perdew,[13] which focuses on satisfaction of exact constraints with minimal parameters and has recently been broadened to consider "appropriate norms" (i.e., systems that semilocal DFAs can, in principle, describe, such as the uniform electron gas and noble gas atoms).[14] There are various reasons for this particular choice of focusing on this type of nonempirical approximations. As noted above, chemisorption energies are critical in determining catalytic behavior. Wellendorff et al.[15] and Duanmu and Truhlar[16] have recently reported on the performance of semiempirical meta-GGAs for predicting adsorption energies at metal surfaces. However, nonempirical functionals are often preferred for solid state calculations; in fact, PBE is the most widely used DFA in materials science.[13] Although nonempirical DFAs yield errors similar or larger to semiempirical functionals for calculations on molecules,[17,18] they often demonstrate broader applicability to solids and systems outside the typical molecular training sets used to parametrize semiempirical DFAs.[19−21] (Contrary to the case of finite systems, for which thousands of accurate data points to benchmark are available,[22] reliable data for training

Table 1. Chemisorption Energies (in eV) Computed with Various Methods Compared to Experimental Data[a]

	GGA			meta-GGA				
	PBE	PBEsol	RPBE	TPSS	revTPSS	SCAN	RTPSS	expt
H/Pt(111)	−2.63	−2.95	−2.53	−2.66	−2.73	−2.80	−2.60	−2.75
H/Ni(111)	−2.89	−3.15	−2.74	−3.02	−3.08	−3.10	−2.95	−2.89
H/Ni(100)	−2.85	−3.11	−2.72	−3.01	−3.04	−3.03	−2.94	−2.82
H/Rh(111)	−2.82	−3.09	−2.68	−2.93	−2.96	−2.99	−2.85	−2.75
H/Pd(111)	−2.79	−3.04	−2.63	−2.91	−2.92	−2.95	−2.78	−2.84
O/Ni(111)	−5.39	−6.00	−4.89	−5.18	−5.20	−5.49	−4.74	−5.13
O/Ni(100)	−5.73	−6.29	−5.25	−5.56	−5.58	−5.83	−5.15	−5.36
O/Pt(111)	−3.78	−4.36	−3.31	−3.55	−3.59	−3.58	−3.13	−3.69
O/Rh(100)	−5.21	−5.78	−4.73	−5.10	−5.13	−5.17	−4.68	−4.45
I/Pt(111)	−2.51	−3.06	−2.09	−2.53	−2.77	−2.74	−2.21	−2.40
NO/Pt(111)	−1.79	−2.22	−1.36	−1.74	−1.67	−2.20	−1.47	−1.23
NO/Pd(111)	−2.29	−2.71	−1.82	−2.32	−2.51	−2.78	−2.00	−1.89
NO/Pd(100)	−2.20	−2.65	−1.76	−2.26	−2.35	−2.66	−1.97	−1.69
CO/Ni(111)	−2.04	−2.54	−1.63	−1.94	−2.19	−2.32	−1.58	−1.28
CO/Pt(111)	−1.63	−1.97	−1.29	−1.47	−1.45	−1.78	−1.23	−1.28
CO/Pd(111)	−1.92	−2.36	−1.49	−1.79	−1.91	−2.10	−1.45	−1.49
CO/Pd(100)	−1.88	−2.26	−1.49	−1.70	−1.74	−1.98	−1.44	−1.63
CO/Rh(111)	−1.91	−2.23	−1.63	−1.76	−1.79	−2.12	−1.55	−1.47
CO/Ir(111)	−1.98	−2.30	−1.71	−1.83	−1.87	−2.16	−1.60	−1.7
CO/Cu(111)	−0.72	−0.95	−0.42	−0.63	−0.67	−0.84	−0.46	−0.59
CO/Ru(0001)	−1.90	−2.22	−1.63	−1.80	−1.82	−2.02	−1.58	−1.67
ME	−0.28	−0.68	0.06	−0.22	−0.28	−0.46	0.03	
MAE	0.30	0.68	0.15	0.24	0.30	0.47	0.18	
median	−0.26	−0.67	0.07	−0.18	−0.21	−0.36	0.05	

[a]ME = mean error (theory−experiment); MAE = mean absolute error.

DOI: 10.1021/acs.jctc.8b00288
J. Chem. Theory Comput. 2018, 14, 3083−3090

empirical functionals on infinite systems is rather scarce.) Thus, we concentrate on benchmarking popular nonempirical meta-GGAs of this school: TPSS,[23] revTPSS,[24] and the more recent SCAN[14] functional. The performance of these functionals is compared to that of the nonempirical GGAs in which they are based (i.e., PBE[7] and PBEsol[25]) and RPBE.[8] Given that we find that none of the GGAs or meta-GGAs outperforms RPBE for chemisorption, we propose a meta-GGA (RTPSS) that is based on RPBE in the same way in which TPSS is based on PBE. The adsorption energies of RTPSS are more accurate than those of other nonempirical meta-GGAs, rivaling those of RPBE. RTPSS also predicts the correct site preference for adsorption of CO on Cu surfaces (a notably difficult problem for semilocal functionals[26−28]) and gives a good description of barrier heights. Thus, we argue that RTPSS can be a useful functional for modeling catalytic heterogeneous reactions.

RESULTS AND DISCUSSION

Chemisorption Energies. We calculated 21 chemisorption energies for a subset of the data set of adsorption energies by Wellendorff et al.[15] (which includes both physisorption and chemisorption data). These calculations were carried out in the Vienna *ab initio* Simulation Package[29] (VASP) using PBE pseudopotentials, a 680 eV plane-wave energy cutoff, and a 4 × 4 × 1 k-mesh grid. The model unit cells are identical to those used in ref 16: a four layer metal slab with at least 10 Å of vacuum separation and an adsorbate coverage of 1/4. The conjugate gradient algorithm was employed for the ionic relaxation; all nuclei in the unit cell were allowed to relax.

The computed and experimental data are collected in Table 1. These energies are purely electronic; contributions from thermal vibrations and zero point energies estimated with the PBE functional have been subtracted from the reference experimental enthalpies.[15] As in ref 16, we report energies for pure chemisorption processes. By this we mean that, for example, in the case of dissociative adsorption of a diatomic molecule A_2 on a metal surface M, we report the chemisorption energy, E_{chem}, for the reaction

$$A + M \rightarrow A/M \quad (E_{chem})$$

calculated as half the difference between the reaction energies for

$$A_2 + 2M \rightarrow 2A/M \quad (E_1)$$

and

$$A_2 \rightarrow 2A \quad (E_2)$$

That is, the chemisorption energy is $E_{chem} = \frac{1}{2}(E_1 - E_2)$. For more details and specific examples, see ref 16.

The mean errors (MEs), mean absolute errors (MAEs), and median of the errors (which is less sensitive to outliers) for each functional are also given in Table 1. In agreement with previous reports in the literature,[8,15,16] PBE and PBEsol predict too negative adsorption energies with MEs of −0.28 and −0.68 eV, respectively, and MAEs similar in magnitude to their MEs. This tendency is corrected by the RPBE functional (ME = 0.06 eV). The results for meta-GGAs mirror those of their GGA counterparts: TPSS, revTPSS, and SCAN all overestimate the stability of the adsorbed species. This overestimation trend is absent in the data calculated with the here proposed RTPSS meta-GGA (ME = 0.03 eV), which transforms the exchange enhancement factor of TPSS in a similar way in which RPBE modifies F_x^{PBE}. That is, the exchange enhancement factor of TPSS is

$$F_x^{TPSS}(x) = 1 + \kappa - \frac{\kappa}{1 + x/\kappa} \quad (5)$$

where x is a function of $p = s^2$ and $z = \tau/\tau^W$, with $\tau^W = \frac{1}{8}|\nabla n|^2/n$ as the single orbital limit of the kinetic energy density, whose leading term is proportional to s^2 (see eq 10 in ref 23). Thus, in analogy with eqs 2 and 4, the exchange enhancement factor of RTPSS is defined as

$$F_x^{RTPSS}(x) = 1 + \kappa(1 - e^{-x/\kappa}) \quad (6)$$

We can expect this transformation to improve chemisorption energies because of two reasons: (1) TPSS has the same tendency as PBE of overbinding adsorbates, whereas RPBE does not. (2) The leading term of $x(p,z)$ is proportional to s^2; therefore, RTPSS can be expected to reduce the stability of adsorbed species as compared to TPSS because of the same reason that RPBE reduces the stability of adsorbed species as compared to PBE (see the Introduction and Figure 2). The

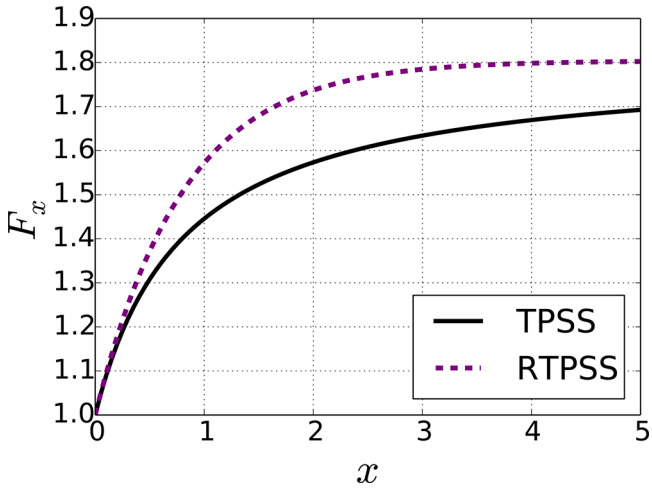

Figure 2. Comparison of the dependence of the exchange enhancement factor on x for TPSS and RTPSS.

results of Table 1 suggest that the overly negative E_{chem} values of TPSS are indeed improved by RTPSS (below, we demonstrate also that such an improvement is statistically significant).

Of course, TPSS was designed to satisfy certain exact constraints, and it is therefore fair to ask whether RTPSS satisfies these constraints. The Lieb−Oxford bound is satisfied because κ stays unchanged, and thus $F_x^{RTPSS} \leq 1.804$. The uniform and slowly varying limits are satisfied because, in these limits, $x \approx 0$ so that both $F_x^{TPSS} \approx 1 + x$ and $F_x^{RTPSS} \approx 1 + x$. Another requirement arises due to the fact that, for a two-electron ground state density ($z = 1$), the exchange potential $v_x = \delta E_x/\delta n$ has a $\nabla^2 n$ term which diverges at a nucleus unless its coefficient vanishes at that point. Because this coefficient is proportional to dF_x/ds and $s = 0.376$ for a two-electron density at a nucleus, such a spurious divergence can be eliminated by satisfying[23]

$$\frac{dF_x(p = s^2, z = 1)}{ds}\Big|_{s=0.376} = 0 \quad (7)$$

DOI: 10.1021/acs.jctc.8b00288
J. Chem. Theory Comput. 2018, 14, 3083−3090

Table 2. Different Error Measures Computed from the Data in Table 1[a]

	GGA			meta-GGA				
error measure	PBE	PBEsol	RPBE	TPSS	revTPSS	SCAN	RTPSS	expt
mean error (eV)	−0.28	−0.68	**0.06**	−0.22	−0.28	−0.46	**0.03**	0.00
mean absolute error (eV)	0.30	0.68	**0.15**	0.24	0.30	0.47	**0.18**	0.00
mean absolute percent error (%)	16.94	36.51	**7.65**	13.46	16.46	26.56	**8.55**	0.00
standard deviation (eV)	0.24	0.32	**0.18**	0.22	0.25	0.31	**0.21**	0.00
median (eV)	−0.26	−0.67	0.07	−0.18	−0.21	−0.36	**0.05**	0.00
median absolute deviation (eV)	0.17	0.26	**0.10**	**0.11**	0.13	0.15	0.14	0.00
interquartile range (eV)	0.34	0.51	**0.18**	**0.23**	0.31	0.41	0.26	0.00
linear fit slope	**0.98**	1.03	0.96	**0.97**	0.96	0.92	0.94	1.00
linear fit intercept (eV)	−0.33	−0.61	**−0.05**	−0.30	−0.38	−0.65	**−0.13**	0.00
Kendall τ_c correlation coeff	0.87	0.84	**0.91**	**0.88**	0.86	0.80	**0.88**	1.00

[a]In each case, the errors from the two functionals closer to experiment are highlighted in bold.

Table 3. Wilcoxon Signed-Rank Test *W* Statistic for the Errors in the Chemisorption Energies of Table 1 for Each Pair of Functionals[a]

	GGA			meta-GGA			
	PBE	PBEsol	RPBE	TPSS	revTPSS	SCAN	RTPSS
PBE		210(0.00)	210(0.00)	111(0.05)	**2(0.69)**	180(0.00)	186(0.00)
PBEsol	210(0.00)		210(0.00)	210(0.00)	210(0.00)	200(0.00)	210(0.00)
RPBE	210(0.00)	210(0.00)		210(0.00)	210(0.00)	210(0.00)	**32(0.36)**
TPSS	111(0.05)	210(0.00)	210(0.00)		173(0.00)	210(0.00)	190(0.00)
revTPSS	**2(0.69)**	210(0.00)	210(0.00)	173(0.00)		196(0.00)	210(0.00)
SCAN	180(0.00)	200(0.00)	210(0.00)	210(0.00)	196(0.00)		210(0.00)

[a]The *p*-values are given in parentheses. Pairs with $W < 58$ and $p > 0.05$ lack statistically significant difference in their results. These pairs are highlighted in bold.

Using the chain rule to differentiate F_x and noting that $x(p,z)$ is identical for TPSS and RTPSS, it is straightforward to prove that

$$\frac{dF_x^{TPSS}}{ds} = 0 \Leftrightarrow \frac{dF_x^{RTPSS}}{ds} = 0 \tag{8}$$

That is, dF_x/ds vanishes in RTPSS if and only if it also vanishes in TPSS. Since TPSS obeys eq 7, RTPSS also satisfies the constraint given by eq 7.

The one constraint satisfied by TPSS but not by RTPSS is the exact exchange energy of the hydrogen atom. Because $F_x^{RTPSS} \geq F_x^{TPSS}$, RTPSS gives an exchange energy that is about 0.14 eV lower than the exact value. Although $x(p,z)$ contains parameters that may be altered to make RTPSS yield the exact H atom energy (without interfering with the satisfaction of other constraints), the net effect of doing this is to make RTPSS so similar to TPSS that the description of chemisorption is not improved. Thus, we opt for the form of F_x^{RTPSS} given in eq 6, even if it breaks this one constraint. The need to break an exact constraint may be due to either the limited form of meta-GGAs or the need for a more complex definition of the exchange enhancement factor. Later in the text, we provide arguments for the limited form of semilocal approximations being responsible for the difficulties in describing adsorption processes.

When comparing the accuracy of quantum chemical methods for calculating a certain property, there are two critical (but often neglected) issues that one must consider. One is the fact that the use of different error measures can lead to different conclusions.[30−32] For example, a functional that gives low mean errors may yield high average percentage errors if relatively large errors occur for small quantities. The second issue is whether or not there is a statistically significant difference between the results of any two methods. For example, if functional *A* has a smaller MAE than functional *B* but the difference is small enough that it could be attributed to random error, then it is inaccurate to claim that *A* is superior to *B*. We address these issues by considering multiple error measures in Table 2 and a Wilcoxon signed-rank test, whose results are summarized in Table 3.

The error measures in Table 2 are designed to gauge not only average errors (such as in the ME, MAE, and percentage errors) but also statistical dispersion (median absolute deviation), variability (interquartile range), qualitative trends (linear fit slope and intercepts and Kendall τ_c correlation coefficient) and also consider robust statistics (measures more resilient to outliers, such as the median and median absolute deviation). Definitions of these error measures may be found in ref 30; we just specify the linear fit and τ_c definitions used here for convenience of the reader. The linear trend is defined as

$$E_{chem}^{expt} = mE_{chem}^{calc} + b \tag{9}$$

Thus, ideally, $m = 1$ and $b = 0$. The Kendall τ_c correlation coefficient is constructed by defining pairs (E_i^{expt}, E_i^{calc}), where E_i^{expt} and E_i^{calc} are the experimental and calculated adsorption energies, respectively. The pairs i and j are then said to be concordant if $E_i^{expt} < E_j^{expt}$ and $E_i^{calc} < E_j^{calc}$, or if $E_i^{expt} > E_j^{expt}$ and $E_i^{calc} > E_j^{calc}$; tied if $E_i = E_j$; and discordant otherwise. The Kendall τ_c is then

$$\tau_c = \frac{P - Q}{\sqrt{(P + Q + T)(P + Q + U)}} \tag{10}$$

where P is the number of concordant pairs, Q is the number of discordant pairs, and T and U the number of ties in the

DOI: 10.1021/acs.jctc.8b00288
J. Chem. Theory Comput. 2018, 14, 3083−3090

experimental and calculated data sets, respectively. Hence, τ gauges the degree of similarity in orderings between two data sets; $\tau = 1$ indicates perfect agreement, whereas $\tau = -1$ indicates complete disagreement. The data in Table 2 clearly supports the idea that RPBE and RTPSS provide the best description of chemisorption energies among the tested functionals.

The degree of statistical difference between the results of any two functionals is quantified in the W statistic and p-values of a Wilcoxon signed-rank test (Table 3). In this test, one analyzes the distribution of the error: the null hypothesis is that the difference between the errors of two functionals follows a symmetric distribution around zero because each set has the same statistical distribution. The null hypothesis is rejected if the test statistic W is greater than a certain W_{crit}, which is determined by the sample size and level of confidence. The p-value associated with the test corresponds to the probability of seeing the observed distribution, or a more asymmetric distribution, assuming that the null hypothesis is true. In the context of comparing quantum chemical approximations, p-values larger than 0.05 are considered to indicate a lack of significant difference in results.[33] In our case, for a 95% confidence interval, $W_{crit} = 58$ so that the results in Table 3 indicate that there are only two pairs of functionals providing essentially the same results: PBE and revTPSS and RPBE and RTPSS. The rest of the pairs show results that are statistically very different. Hence, the conclusion that RPBE and RTPSS provide the best results for chemisorption energies is statistically significant.

It is notable from the results in Tables 1−3 that the functionals that perform better and/or were designed specifically for solids (PBEsol, revTPSS, SCAN) have the largest errors in chemisorption energies. Indeed, PBEsol and revTPSS improve the lattice constants and surface energies of solids relative to PBE and TPSS, respectively.[24,25] The more recent SCAN meta-GGA, which satisfies the most exact constraints and performs well for solids, molecules, and weak interactions,[14] gives larger errors for E_{chem} than TPSS and revTPSS. That is, satisfying more exact constraints leads to worse chemisorption energies. Indeed, as noted above, RTPSS needs to break one exact constraint of TPSS (the H atom exchange energy) to improve E_{chem} values. We therefore suspect that the reason for which semilocal functionals struggle to describe chemisorption is due to inherent limitations in their form.

Adsorption of Carbon Monoxide on Copper. The adsorption of carbon monoxide on copper is a challenging problem for semilocal functionals. While *GW* methods, the random-phase approximation, DFT+U, and hybrid functionals correctly predict the experimentally observed preference of CO to adsorb on top sites of copper surfaces, GGAs tend to prefer adsorption at bridge and hollow sites.[26−28] Moreover, the problem of CO adsorption on copper is relevant in mechanistic studies of CO_2 reduction to useful products such as, e.g., ethanol and ethylene: copper is the only monometallic catalyst that reduces CO_2 to C_2 products with substantial Faradaic efficiency,[34,35] and CO is known to be a key reaction intermediate.[36−39] However, the mechanism by which CO is reduced is highly complex, and the adsorption site of CO can determine whether CO reduces preferentially to CHO or to COH.[40] This in turn can affect how the rest of the mechanism is predicted to unfold.

We consider two facets of a copper surface for which experimental data are available: the (111) and (100) facets.[15,16,41,42] The possible adsorption sites for these surfaces are illustrated in Figure 3. Tables 4 and 5 show the CO adsorption energies predicted by each functional for the different adsorption sites in Cu(111) and Cu(100), respectively. For the Cu(111) facet, all functionals except for RPBE and RTPSS fail to predict the correct adsorption site. In the case of the Cu(100) surface, only RTPSS gives the correct adsorption site (albeit the energy difference between the top,

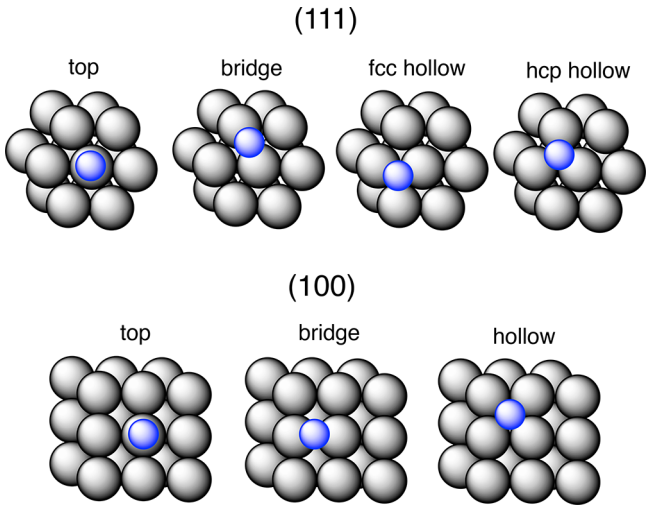

Figure 3. Schematic representation of the different adsorption sites on (111) and (100) facets of a metal surface.

Table 4. Adsorption of Energies of CO on the Different Sites of a Cu(111) Surface[a]

	E_{chem}/eV			
functional	top	bridge	fcc hollow	hcp hollow
PBE	−0.72	−0.72	−0.70	**−0.80**
PBEsol	−0.95	−1.10	−1.18	**−1.21**
RPBE	**−0.42**	−0.39	−0.37	−0.40
TPSS	−0.63	−0.68	−0.70	**−0.71**
revTPSS	−0.67	−0.75	**−0.77**	**−0.77**
SCAN	−0.84	−0.87	**−0.96**	−0.87
RTPSS	**−0.46**	−0.42	−0.43	−0.41
expt	**−0.59**[15]			

[a]Preferred sites are highlighted in bold.

Table 5. Adsorption of Energies of CO on the Different Sites of a Cu(100) Surface[a]

	E_{chem}/eV		
functional	top	bridge	hollow
PBE	−0.72	−0.75	**-0.85**
PBEsol	−1.05	−1.15	**−1.30**
RPBE	−0.46	−0.45	**−0.47**
TPSS	−0.71	−0.69	**−0.74**
revTPSS	−0.74	−0.75	**−0.86**
SCAN	−0.90	−0.96	**−1.04**
RTPSS	**-0.52**	−0.48	−0.48
expt	**−0.53**,[41] **−57**[42]		

[a]Preferred sites are highlighted in bold.

DOI: 10.1021/acs.jctc.8b00288
J. Chem. Theory Comput. 2018, 14, 3083−3090

bridge, and hollow sites in RPBE is very small). In addition, the E_{chem} values of RTPSS are in good agreement with experiment in both cases. This is not true for all functionals; in the most extreme case, the errors of the PBEsol GGA are more than half an electronvolt. These results reinforce the observations in the previous section that indicate RTPSS to be a robust functional for modeling chemisorption processes. Given the importance of adsorption modes in determining intermediates involved in the reduction of CO_2 on metal surfaces, RTPSS may be a promising method for modeling such catalytic reactions.

Other Properties: Atomization Energies and Reaction Barriers. While we have focused on chemisorption processes due to their importance in heterogeneous catalysis, it is interesting to see how RTPSS fares in the calculation of other properties. We thus take a brief look at two properties of interest in the study of RTPSS: atomization energies (AEs) and hydrogen transfer barrier heights (HTBHs). Atomization energies are interesting because they correlate with the strength of intramolecular bonds, just like chemisorption energies correlate with the strength of the chemical interaction between an atom or molecule and a surface. Additionally, AEs have historically been used to benchmark electronic structure methods, although their adequacy as a metric for the quality of many-body approximations has been questioned in recent years due to the fact that AEs are not size-intensive, resulting in errors of approximate methods increasing linearly with increasing molecular size.[31,43] Hydrogen transfer reaction barriers are interesting too because such processes are relevant in important catalytic reactions such as the hydrogen evolution reaction and the CO_2 reduction reaction.

The AE6 and BH6 data sets of Lynch and Truhlar[44] are ideal for taking a quick glance at the performance of RTPSS for calculating AEs and HTBHs. We carried out calculations for the systems comprising these data sets in VASP with a plane-wave energy cutoff of 1024 eV. Table 6 compiles the MEs and MAEs

Table 6. Mean Errors (MEs) and Mean Absolute Errors (MAEs) Given by Different Functionals for the AE6 (Atomization Energies), IAE6 (Intensive Atomization Energies), and BH6 (Barrier Heights) Data Sets[a]

	AE6		IAE6		BH6	
functional	ME	MAE	ME	MAE	ME	MAE
PBE	0.87	1.02	0.20	0.23	−0.46	0.46
PBEsol	1.56	1.58	0.28	0.29	−0.55	0.55
RPBE	−0.35	0.42	−0.05	0.08	−0.28	0.28
TPSS	0.12	0.23	0.02	0.06	−0.32	0.32
revTPSS	0.09	0.28	0.01	0.08	−0.28	0.28
SCAN	−0.02	0.15	−0.01	0.05	−0.33	0.33
RTPSS	−0.68	0.77	−0.12	0.14	−0.22	0.23

[a]All values are in eV.

that the different functionals tested here give for these data sets. In addition, we include results for a data set for intensive atomization energies[31,43] (IAEs) constructed from the AE6 data set (IAE6). IAEs are defined as the atomization energy per atom, i.e.

$$\mathrm{IAE} = \mathrm{AE}/N_{at} \tag{11}$$

where N_{at} is the number of atoms in the system. The reason for considering IAEs is to avoid the aforementioned problem of errors in AEs growing uncontrolled with system size.

Interestingly, the results from meta-GGAs for AEs are, in a sense, reversed from the results for chemisorption: for AEs, SCAN has the smallest errors while RTPSS has the largest. The RTPSS MAE for the AE6 data set is rather large (0.77 eV); however, the MAE for the IAE6 data set is much smaller and within the range of typical errors from semilocal DFAs (0.14 eV). This suggests that RTPSS can provide a reasonable description of bond breaking processes (as long as only one or two bonds are involved). Furthermore, RTPSS gives the smallest errors for the BH6 data set of reaction barriers. It is worth noting that self-interaction error is responsible for both the too-low reaction barriers given by semilocal DFAs and the failure of these approximations to correctly describe CO adsorption on metal surfaces. These observations suggest that the exchange enhancement factor of RTPSS reduces self-interaction relative to other meta-GGAs (as we have seen above, among meta-GGAs, RTPSS provides the best results for CO adsorption). Indeed, the fact that $F_x^{\mathrm{TPSS}} \leq F_x^{\mathrm{RTPSS}}$ leads to increased (negative) exchange can be expected to reduce self-repulsion in RTPSS as compared to TPSS.

Accurate DFAs for Chemisorption May Fail for Physisorption. While we do not attempt here to make a comprehensive benchmarking of nonempirical meta-GGAs for physisorption, we provide an example to caution that semilocal DFAs that are accurate for chemisorption may fail to describe physisorption. The example we use is that of benzene adsorbing on an Ag(111) surface (Figure 4). Table 7 lists the calculated

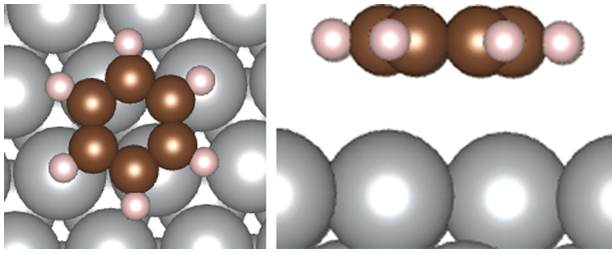

Figure 4. Model for benzene physisorbed on an Ag(111) surface.

and experimental physisorption energies (E_{phys}) for this process (the reference energy is also taken from the data set of Wellendorff et al.[15]). All of the functionals give too-positive E_{phys} values as compared with experiment (−0.63 eV); SCAN gives the closest result at −0.27 eV, while RPBE is farthest from experiment at +0.28 eV. RTPSS fares better than RPBE but still does not even predict a negative adsorption energy (+0.10 eV). In fact, the results for C_6H_6/Ag(111) are completely opposed to the trends seen for chemisorption: the errors tend to be positive, and SCAN and PBEsol energies have the smallest errors, whereas RTPSS and RPBE energies have the largest.

The reason for this failure of semilocal DFAs to describe physisorption is simple: long-range interactions become more important than in chemisorption, but semilocal functionals cannot describe long-range correlation properly.[45] (It is also for this reason that SCAN, which has been shown to be better at describing weak interactions than TPSS,[14] gives the best result in this case.) The upside of this is that the inadequacy of semilocal functionals for capturing long-range interactions has long been well-known to the DFT community, and strategies have been developed to tackle the problem.[17,18] Functionals that incorporate nonlocal correlation in addition to semilocal correlation can describe long-range interactions. Examples of

DOI: 10.1021/acs.jctc.8b00288
J. Chem. Theory Comput. 2018, 14, 3083−3090

Table 7. Adsorption Energies (in eV) for Benzene on Ag(111) Computed with Various Methods and Compared to Experimental Data

	GGA			meta-GGA				
	PBE	PBEsol	RPBE	TPSS	revTPSS	SCAN	RTPSS	expt
E_{phys}	−0.07	−0.18	0.28	0.03	0.09	−0.27	0.10	−0.63[15]

meta-GGAs in this category include mBEEF-vdW,[46] B97M-V,[22] and SCAN+rVV10.[47] The rVV10 correlation functional in particular was designed for efficient evaluation in extended solids.[48] Thus, a combination of RTPSS with rVV10 could be a promising alternative for describing chemisorption and physisorption accurately with a single functional.

CONCLUSIONS

We benchmarked popular nonempirical semilocal DFAs for the calculation of chemisorption energies at metal surfaces. All of the tested meta-GGAs tend to give too-negative chemisorption energies; we then developed a new meta-GGA, RTPSS, that remedies this issue and improves the description of chemisorption processes. RTPSS is based on the RPBE GGA in the same way that TPSS is based on PBE—RPBE was designed to improve the poor predictions of E_{chem} values of PBE, and RTPSS works for similar reasons. Among the tested functionals, RPBE and RTPSS provide the most accurate description of chemisorption processes. The fact that RTPSS also improves the accuracy of hydrogen transfer barrier heights suggests diminished self-interaction in this functional as compared to other tested meta-GGAs. Therefore, we believe that RTPSS can be a useful functional for computational heterogeneous catalysis.

Nonetheless, the limitations of semilocal approximations also show in our results. The functionals giving the best description of chemisorption provide are the least accurate for physisorption and atomization energies and vice versa. SCAN, which satisfies the most exact constraints of any DFA studied here, performs best for the latter properties but gives worse results than TPSS and revTPSS for chemisorption. This suggests that, in spite of being at the top of Jacob's ladder of semilocal functionals, the limited form of meta-GGAs may prevent them from simultaneously describing all of these properties accurately. A clear shortcoming is the poor description of van der Waals forces, which are important in physisorption processes. Nevertheless, inclusion of nonlocal correlation using well-established techniques can remedy this issue. Thus, a functional such as, e.g., RTPSS+rVV10 would be a promising candidate for treating complex systems involving both chemisorption and physisorption.

AUTHOR INFORMATION

Corresponding Authors

*E-mail: alexbell@berkeley.edu.

*E-mail: mhg@cchem.berkeley.edu.

ORCID

Alejandro J. Garza: 0000-0001-6995-2833

Alexis T. Bell: 0000-0002-5738-4645

Martin Head-Gordon: 0000-0002-4309-6669

Funding

This material is based on work performed in the Joint Center for Artificial Photosynthesis, a DOE Energy Innovation Hub, supported through the Office of Science of the U.S. Department of Energy under Award DE-SC0004993. This research used resources of the National Energy Research Scientific Computing Center, a DOE Office of Science User Facility supported by the Office of Science of the U.S. Department of Energy under Contract No. DE-AC02-05CH11231.

Notes

The authors declare no competing financial interest.

ACKNOWLEDGMENTS

We thank Prof. Jianwei Sun for sharing VASP subroutines for the SCAN functional with us.

REFERENCES

(1) Kortlever, R.; Shen, J.; Schouten, K. J. P.; Calle-Vallejo, F.; Koper, M. T. M. Catalysts and Reaction Pathways for the Electrochemical Reduction of Carbon Dioxide. *J. Phys. Chem. Lett.* **2015**, *6*, 4073−4082.

(2) Laursen, A. B.; Man, I. C.; Trinhammer, O. L.; Rossmeisl, J.; Dahl, S. The Sabatier principle illustrated by catalytic H_2O_2 decomposition on metal surfaces. *J. Chem. Educ.* **2011**, *88*, 1711−1715.

(3) Medford, A. J.; Vojvodic, A.; Hummelshøj, J. S.; Voss, J.; Abild-Pedersen, F.; Studt, F.; Bligaard, T.; Nilsson, A.; Nørskov, J. K. From the Sabatier principle to a predictive theory of transition-metal heterogeneous catalysis. *J. Catal.* **2015**, *328*, 36−42.

(4) Paier, J.; Marsman, M.; Hummer, K.; Kresse, G. Screened hybrid density functionals applied to solids. *J. Chem. Phys.* **2006**, *124*, 154709.

(5) Tran, F.; Koller, D.; Blaha, P. Application of screened hybrid functionals to the bulk transition metals Rh, Pd, and Pt. *Phys. Rev. B: Condens. Matter Mater. Phys.* **2012**, *86*, 134406.

(6) Gao, W.; Abtew, T. A.; Cai, T.; Sun, Y.-Y.; Zhang, S.; Zhang, P. On the applicability of hybrid functionals for predicting fundamental properties of metals. *Solid State Commun.* **2016**, *234-235*, 10−13.

(7) Perdew, J. P.; Burke, K.; Ernzerhof, M. Generalized Gradient Approximation Made Simple. *Phys. Rev. Lett.* **1996**, *77*, 3865−3868.

(8) Hammer, B.; Hansen, L. B.; Nørskov, J. K. Improved adsorption energetics within density-functional theory using revised Perdew-Burke-Ernzerhof functionals. *Phys. Rev. B: Condens. Matter Mater. Phys.* **1999**, *59*, 7413−7421.

(9) Lieb, E. H. A lower bound for Coulomb energies. *Phys. Lett. A* **1979**, *70*, 444−446.

(10) Lieb, E. H.; Oxford, S. Improved lower bound on the indirect Coulomb energy. *Int. J. Quantum Chem.* **1981**, *19*, 427−439.

(11) Garza, A. J.; Scuseria, G. E.; Ruzsinszky, A.; Sun, J.; Perdew, J. P. The two pillars: density and spin-density functional theories. *Mol. Phys.* **2016**, *114*, 928−931.

(12) Sun, J.; Xiao, B.; Fang, Y.; Haunschild, R.; Hao, P.; Ruzsinszky, A.; Csonka, G. I.; Scuseria, G. E.; Perdew, J. P. Density functionals that recognize covalent, metallic, and weak bonds. *Phys. Rev. Lett.* **2013**, *111*, 106401.

(13) Burke, K. Perspective on density functional theory. *J. Chem. Phys.* **2012**, *136*, 150901.

(14) Sun, J.; Ruzsinszky, A.; Perdew, J. P. Strongly Constrained and Appropriately Normed Semilocal Density Functional. *Phys. Rev. Lett.* **2015**, *115*, 036402.

(15) Wellendorff, J.; Silbaugh, T. L.; Garcia-Pintos, D.; Nørskov, J. K.; Bligaard, T.; Studt, F.; Campbell, C. T. A Benchmark Database for Adsorption Bond Energies to Transition Metal Surfaces and Comparison to Selected DFT Functionals. *Surf. Sci.* **2015**, *640*, 36−44.

(16) Duanmu, K.; Truhlar, D. G. Validation of Density Functionals for Adsorption Energies on Transition Metal Surfaces. *J. Chem. Theory Comput.* **2017**, *13*, 835−842.

DOI: 10.1021/acs.jctc.8b00288
J. Chem. Theory Comput. 2018, 14, 3083−3090

(17) Goerigk, L.; Hansen, A.; Bauer, C.; Ehrlich, S.; Najibi, A.; Grimme, S. A look at the density functional theory zoo with the advanced GMTKN55 database for general main group thermochemistry, kinetics and noncovalent interactions. *Phys. Chem. Chem. Phys.* **2017**, *19*, 32184−32215.
(18) Mardirossian, N.; Head-Gordon, M. Thirty years of density functional theory in computational chemistry: an overview and extensive assessment of 200 density functionals. *Mol. Phys.* **2017**, *115*, 2315−2372.
(19) Kurth, S.; Perdew, J. P.; Blaha, P. Molecular and solid-state tests of density functional approximations: LSD, GGAs, and meta-GGAs. *Int. J. Quantum Chem.* **1999**, *75*, 889−909.
(20) Ahlrichs, R.; Furche, F.; Grimme, S. Comment on "Assessment of exchange correlation functionals. *Chem. Phys. Lett.* **2000**, *325*, 317−321.
(21) Paier, J.; Marsman, M.; Kresse, G. Why does the B3LYP hybrid functional fail for metals? *J. Chem. Phys.* **2007**, *127*, 024103.
(22) Mardirossian, N.; Head-Gordon, M. Mapping the genome of meta-generalized gradient approximation density functionals: The search for B97M-V. *J. Chem. Phys.* **2015**, *142*, 074111.
(23) Tao, J.; Perdew, J. P.; Staroverov, V. N.; Scuseria, G. E. Climbing the Density Functional Ladder: Non-Empirical Meta-Generalized Gradient Approximation Designed for Molecules and Solids. *Phys. Rev. Lett.* **2003**, *91*, 146401.
(24) Perdew, J. P.; Ruzsinszky, A.; Csonka, G. I.; Constantin, L. A.; Sun, J. Workhorse Semilocal Density Functional for Condensed Matter Physics and Quantum Chemistry. *Phys. Rev. Lett.* **2009**, *103*, 026403.
(25) Perdew, J. P.; Ruzsinszky, A.; Csonka, G. I.; Vydrov, O. A.; Scuseria, G. E.; Constantin, L. A.; Zhou, X.; Burke, K. Restoring the Density-Gradient Expansion for Exchange in Solids and Surfaces. *Phys. Rev. Lett.* **2008**, *100*, 136406.
(26) Gajdos, M.; Hafner, J. CO Adsorption on Cu(111) and Cu(001) Surfaces: Improving Site Preference in DFT Calculations. *Surf. Sci.* **2005**, *590*, 117−126.
(27) Stroppa, A.; Termentzidis, K.; Paier, J.; Kresse, G.; Hafner, J. CO adsorption on metal surfaces: A hybrid functional study with plane-wave basis set. *Phys. Rev. B: Condens. Matter Mater. Phys.* **2007**, *76*, 195440.
(28) Ren, X.; Rinke, P.; Scheffler, M. Exploring the random phase approximation: Application to CO adsorbed on Cu (111). *Phys. Rev. B: Condens. Matter Mater. Phys.* **2009**, *80*, 045402.
(29) Kresse, G.; Furthmüller, J. Efficient iterative schemes for ab initio total-energy calculations using a plane-wave basis set. *Phys. Rev. B: Condens. Matter Mater. Phys.* **1996**, *54*, 11169.
(30) Civalleri, B.; Presti, D.; Dovesi, R.; Savin, A. On Choosing the Best Density Functional Approximation. *Chem. Modell.* **2012**, *9*, 168−185.
(31) Savin, A.; Johnson, E. Judging Density-Functional Approximations: Some Pitfalls of Statistics. *Top. Curr. Chem.* **2014**, *365*, 81−96.
(32) Garza, A. J.; Scuseria, G. E. Predicting Band Gaps with Hybrid Density Functionals. *J. Phys. Chem. Lett.* **2016**, *7*, 4165−4170.
(33) Skone, J. H.; Govoni, M.; Galli, G. Nonempirical Range-Separated Hybrid Functionals for Solids and Molecules. *Phys. Rev. B: Condens. Matter Mater. Phys.* **2016**, *93*, 235106.
(34) Hori, Y. Electrochemical CO_2 Reduction on Metal Electrodes. In *Modern Aspects of Electrochemistry*; Springer: New York, 2008; pp 89−189, DOI: DOI: 10.1007/978-0-387-49489-0_3.
(35) Kuhl, K. P.; Cave, E. R.; Abram, D. N.; Jaramillo, T. F. New insights into the electrochemical reduction of carbon dioxide on metallic copper surfaces. *Energy Environ. Sci.* **2012**, *5*, 7050−7059.
(36) Schouten, K. J. P.; Kwon, Y.; van der Ham, C. J. M.; Qin, Z.; Koper, M. T. M. A new mechanism for the selectivity to C1 and C2 species in the electrochemical reduction of carbon dioxide on copper electrodes. *Chem. Sci.* **2011**, *2*, 1902−1909.
(37) Hori, Y.; Murata, A.; Takahashi, R.; Suzuki, S. Electroreduction of carbon monoxide to methane and ethylene at a copper electrode in aqueous solutions at ambient temperature and pressure. *J. Am. Chem. Soc.* **1987**, *109*, 5022−5023.
(38) Hori, Y.; Takahashi, R.; Yoshinami, Y.; Murata, A. Electrochemical Reduction of CO at a Copper Electrode. *J. Phys. Chem. B* **1997**, *101*, 7075−7081.
(39) Gattrell, M.; Gupta, N.; Co, A. A review of the aqueous electrochemical reduction of CO2 to hydrocarbons at copper. *J. Electroanal. Chem.* **2006**, *594*, 1−19.
(40) Garza, A. J.; Bell, A. T.; Head-Gordon, M. Mechanism of CO_2 Reduction at Copper Surfaces: Pathways to C_2 Products. *ACS Catal.* **2018**, *8*, 1490−1499.
(41) Vollmer, S.; Witte, G.; Wöll, C. Determination of site specific adsorption energies of CO on copper. *Catal. Lett.* **2001**, *77*, 97−101.
(42) Tracy, J. C. Structural influences on adsorption energy. II. CO on Ni (100). *J. Chem. Phys.* **1972**, *56*, 2736−2747.
(43) Perdew, J. P.; Sun, J.; Garza, A. J.; Scuseria, G. E. Intensive Atomization Energy: Re-Thinking a Metric for Electronic Structure Theory Methods. *Z. Phys. Chem.* **2016**, *230*, 737−742.
(44) Lynch, B. J.; Truhlar, D. G. Small Representative Benchmarks for Thermochemical Calculations. *J. Phys. Chem. A* **2003**, *107*, 8996−8999.
(45) Ambrosetti, A.; Reilly, A. M.; DiStasio, R. A., Jr.; Tkatchenko, A. Long-range correlation energy calculated from coupled atomic response functions. *J. Chem. Phys.* **2014**, *140*, 18A508.
(46) Lundgaard, K. T.; Wellendorff, J.; Voss, J.; Jacobsen, K. W.; Bligaard, T. mBEEF-vdW: Robust fitting of error estimation density functionals. *Phys. Rev. B: Condens. Matter Mater. Phys.* **2016**, *93*, 235162.
(47) Peng, H.; Yang, Z. H.; Perdew, J. P.; Sun, J. Versatile van der Waals density functional based on a meta-generalized gradient approximation. *Phys. Rev. X* **2016**, *6*, 041005.
(48) Sabatini, R.; Gorni, T.; de Gironcoli, S. Nonlocal van der Waals density functional made simple and efficient. *Phys. Rev. B: Condens. Matter Mater. Phys.* **2013**, *87*, 041108.

DOI: 10.1021/acs.jctc.8b00288
J. Chem. Theory Comput. 2018, 14, 3083−3090